

See discussions, stats, and author profiles for this publication at: <https://www.researchgate.net/publication/11046920>

# Dissociative Electron Transfer to Haloacetonitriles. An Example of the Dependency of In-Cage Ion-Radical Interactions upon the Leaving Group

ARTICLE *in* JOURNAL OF THE AMERICAN CHEMICAL SOCIETY · DECEMBER 2002

Impact Factor: 12.11 · DOI: 10.1021/ja0275212 · Source: PubMed

---

CITATIONS

76

---

READS

35

5 AUTHORS, INCLUDING:



Armando Gennaro

University of Padova

106 PUBLICATIONS 2,754 CITATIONS

SEE PROFILE



Marc Robert

Paris Diderot University

113 PUBLICATIONS 2,754 CITATIONS

SEE PROFILE

## Dissociative Electron Transfer to Haloacetonitriles. An Example of the Dependency of In-Cage Ion-Radical Interactions upon the Leaving Group

Annarita Cardinale,<sup>1a</sup> Abdirisak A. Isse,<sup>1a</sup> Armando Gennaro,<sup>\*,1a</sup> Marc Robert,<sup>1b</sup> and Jean-Michel Savéant<sup>\*,1b</sup>

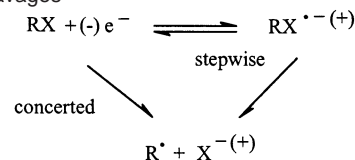
Contribution from the Dipartimento di Chimica Fisica, Università di Padova, via Loredan 2, 35131 Padova, Italy, and Laboratoire d'Electrochimie Moléculaire, Université de Paris 7 - Denis Diderot, Case Courrier 7107, 2 place Jussieu, 75251 Paris Cedex 05, France

Received July 1, 2002

**Abstract:** The reductive cleavage of the haloacetonitriles (Cl, Br, I) in DMF provides additional examples of the formation of a fragment cluster upon dissociative electron transfer, which is able to survive in this polar solvent thanks to the electron-withdrawing character of the cyano group. The remarkable sensitivity of the activation energy to small changes of the interaction energies allows, with help of the "sticky" dissociative electron-transfer model, the precise determination of interaction energies down to a few millielectronvolts from the cyclic voltammetric data. The interaction energy rapidly decreases from Cl to Br and to I, correlated with the increase of the halide radius. These observations add to the previously gathered evidence to confirm the existence of such interactions and to highlight their electrostatic character. This is further corroborated by the quantum chemical computation of the potential energy profiles, which exhibit a long-distance energy minimum. This revisiting of the notion of  $\sigma$ -ion radicals and of their status in a polar medium makes them appear as an electrostatic radical-ion pair rather than covalently bound molecules. Their stability is a function of the Lewis acid–base properties of both the radical and the leaving ion and is strongly influenced by the nature of the solvent.

Starting from a neutral closed-shell molecule, an ion and a radical are the products of the one-electron reductive or oxidative cleavage of neutral molecules whether it follows a concerted or a stepwise pathway (Scheme 1), no matter the mode of injection or removal of the electron, thermal (electrochemical or homogeneous) or photoinduced.<sup>2–10</sup>

**Scheme 1.** Concerted and Stepwise Mechanisms in Reductive or Oxidative Cleavages



The question arises whether the two fragments may form a significantly stable cluster. Quantum chemical estimates of the interaction between the two fragments in the gas phase reveal that it may be substantial.<sup>11,12,13a</sup> For example, the energy of the interaction between  $\text{CCl}_3^{\bullet}$  and  $\text{Cl}^-$  has been found to be on

\* To whom correspondence should be addressed. E-mail: saveant@paris7.jussieu.fr.

- (1) (a) Università di Padova. (b) Université de Paris 7 – Denis Diderot.
- (2) (a) Savéant, J.-M. Electron Transfer, Bond Breaking, and Bond Formation. In *Advances in Physical Organic Chemistry*; Tidwell, T. T., Ed.; Academic Press: New York, 2000; Vol. 35, pp 117–192. (b) Hush, N. S. *J. Electroanal. Chem.* **1999**, 470, 170. (c) Malet, Y. A.; Cannon, R. D. *Theor. Exp. Chem.* **1998**, 34, 7. (d) Lund, H.; Daasbjerg, K.; Lund, T.; Occhialini, D.; Pedersen, S. U. *Acta Chem. Scand.* **1997**, 51, 135. (e) Lund, H.; Daasbjerg, K.; Lund, T.; Pedersen, S. U. *Acc. Chem. Res.* **1995**, 28, 313. (f) Savéant, J.-M. Dissociative Electron Transfer. In *Advances in Electron-Transfer Chemistry*; Mariano, P. S., Ed.; JAI Press: New York, 1994; Vol. 4., pp 53–116. (g) Savéant, J.-M. *Acc. Chem. Res.* **1993**, 26, 455. (h) Savéant, J.-M. Single Electron Transfer and Nucleophilic Substitution. In *Advances in Physical Organic Chemistry*; Bethel, D., Ed.; Academic Press: New York, 1990; Vol. 26, pp 1–130.
- (3) (a) Andrieux, C. P.; Le Gorand, A.; Savéant, J.-M. *J. Am. Chem. Soc.* **1992**, 114, 6892. (b) Andrieux, C. P.; Differding, E.; Robert, M.; Savéant, J.-M. *J. Am. Chem. Soc.* **1993**, 115, 6592. (c) Andrieux, C. P.; Robert, M.; Saeva, F. D.; Savéant, J.-M. *J. Am. Chem. Soc.* **1994**, 116, 7864. (d) Andrieux, C. P.; Tallec, A.; Tardivel, R.; Savéant, J.-M.; Tardy, C. *J. Am. Chem. Soc.* **1997**, 119, 2420.
- (4) (a) Workentin, M. S.; Maran, F.; Wayner, D. D. M. *J. Am. Chem. Soc.* **1995**, 117, 2120. (b) Andersen, M. L.; Mathivanan, N.; Wayner, D. D. M. *J. Am. Chem. Soc.* **1996**, 118, 4871. (c) Andersen, M. L.; Long, W.; Wayner, D. D. M. *J. Am. Chem. Soc.* **1997**, 119, 6590. (d) Antonello, S.; Musumeci, M.; Wayner, D. D. M.; Maran, F. *J. Am. Chem. Soc.* **1997**, 119, 9541. (e) Antonello, S.; Maran, F. *J. Am. Chem. Soc.* **1997**, 119, 12595. (f) Antonello, S.; Maran, F. *J. Am. Chem. Soc.* **1998**, 120, 5713. (g) Workentin, M. S.; Donkers, R. L. *J. Am. Chem. Soc.* **1998**, 120, 2664.

- (5) (a) Maslak, P.; Guthrie, R. D. *J. Am. Chem. Soc.* **1986**, 108, 2628. (b) Maslak, P.; Guthrie, R. D. *J. Am. Chem. Soc.* **1986**, 108, 2637. (c) Maslak, P.; Asel, S. L. *J. Am. Chem. Soc.* **1988**, 110, 8260. (d) Maslak, P.; Narvaez, J. N. *J. Chem. Soc., Chem. Commun.* **1989**, 110, 138. (e) Maslak, P.; Chapman, W. H. *J. Chem. Soc., Chem. Commun.* **1989**, 110, 1809. (f) Maslak, P.; Narvaez, J. N. *Angew. Chem., Int. Ed. Engl.* **1990**, 29, 283. (g) Maslak, P.; Chapman, W. H. *Tetrahedron* **1990**, 46, 2715. (h) Maslak, P.; Chapman, W. H. *J. Org. Chem.* **1990**, 55, 6334. (i) Maslak, P.; Kula, J.; Chateaneuf, J. E. *J. Am. Chem. Soc.* **1991**, 113, 2304. (j) Maslak, P.; Kula, J. *Mol. Cryst. Liq. Cryst.* **1991**, 194, 293. (k) Vallombroso, T. M.; Chapman, W. H.; Narvaez, J. N. *Angew. Chem., Int. Ed. Engl.* **1994**, 33, 73. (l) Maslak, P.; Chapman, W. H.; Vallombroso, T. M. *J. Am. Chem. Soc.* **1995**, 117, 12373. (m) Maslak, P.; Narvaez, J. N.; Vallombroso, T. M.; Watson, B. A. *J. Am. Chem. Soc.* **1995**, 117, 12380. (n) Maslak, P.; McGuin, J. M. *J. Chem. Soc., Chem. Commun.* **1999**, 2467.
- (6) (a) Andrieux, C. P.; Savéant, J.-M. *J. Electroanal. Chem.* **1986**, 205, 43. (b) Pause, L.; Robert, M.; Savéant, J.-M. *J. Am. Chem. Soc.* **1999**, 121, 7158. (c) Antonello, S.; Maran, F. *J. Am. Chem. Soc.* **1999**, 121, 9668.
- (7) (a) Severin, M. G.; Farnia, G.; Vianello, E.; Arévalo, M. C. *J. Electroanal. Chem.* **1988**, 251, 369. (b) Costentin, C.; Hapiot, P.; Médebielle, M.; Savéant, J.-M. *J. Am. Chem. Soc.* **1999**, 121, 4451.

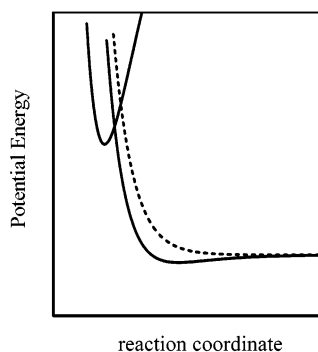


**Figure 1.** Potential energy curves for bond cleavage and bond formation with (full line) and without (dotted line) interaction between the fragments.

the order of 400 meV,<sup>13a</sup> while, for para-substituted benzyl radicals and  $\text{Cl}^-$ , it varies from 200 to 250, 700, and 950 meV in the series  $\text{OCH}_3$ , H, CN,  $\text{NO}_2$ ,<sup>13d</sup> corresponding to carbon–chlorine distances on the order of 2.5–3 Å. These interactions may be so strong as to support the notion of  $\sigma$ -ion radicals (or equivalently of three- or one-electron bonds) in the gas phase<sup>12a</sup> or in apolar solid matrixes.<sup>12b,c</sup>

These interactions are expected to decrease or even to disappear in the liquid phase, particularly in polar solvents. There is, however, growing evidence that this is not necessarily the case, even in solvents as polar as *N,N'*-dimethylformamide (DMF) or acetonitrile, at least when the presence of electron-withdrawing groups induces a positive charge density on the radical atom center that favors its interaction with the counteranion.<sup>13</sup>

The existence and magnitude of these interactions strongly influence the dynamics of the dissociative electron transfer to or from the parent molecule. The increase of the cleavage reactivity due to the interaction has been modeled by means of an extension of the original dissociative electron-transfer theory.<sup>13a–c</sup> As recalled on Figure 1, the contribution of bond

cleavage and bond formation to the potential energy curves describing the reactant and product systems consists, when the interactions between the ion and the radical are negligible,<sup>14</sup> of a Morse curve and repulsive Morse curve (dotted line in Figure 1), respectively.

Under these conditions, the activation free energy,  $\Delta G^\ddagger$ , is related to the reaction standard free energy,  $\Delta G^\circ$ , according to eq 1:

$$\Delta G^\ddagger = \frac{D_R + \lambda_0}{4} \left( 1 + \frac{\Delta G^\circ}{D_R + \lambda_0} \right)^2 \quad (1)$$

where  $D_R$  is the bond dissociation energy of the reactant  $\text{RX}$ , and  $\lambda_0$  is the solvent reorganization energy.

When fragment clustering is significant, the repulsive potential energy profile of the product system is replaced by a complete Morse curve (full line in Figure 1) based on the interaction energy in the radical-ion pair,  $D_P$ . It follows that<sup>13</sup>

$$\Delta G^\ddagger = \frac{(\sqrt{D_R} - \sqrt{D_P})^2 + \lambda_0}{4} \left[ 1 + \frac{\Delta G^\circ - D_P}{(\sqrt{D_R} - \sqrt{D_P})^2 + \lambda_0} \right]^2 \quad (2)$$

As seen in Figure 1 and eq 2, one reason that fragment clustering has a strong influence on the reaction kinetics is that it does not merely modify the driving force, as would a product work term, but also that it decreases the intrinsic barrier (standard activation energy). In this respect, the interference of  $D_P$  through its square root makes it particularly effective. For example, even when  $D_P$  is only 1% of  $D_R$ , thus seeming completely negligible at first sight, its effect on the contribution of bond breaking to the intrinsic barrier is as large as a 15% decrease, that is, perfectly detectable at the experimental level. Evidence for the existence of such ion/radical pairs in polar solvents has been gathered recently thanks to the application of this “sticky” dissociative electron-transfer model, taking advantage of this sensitivity of the reaction kinetics to small values of the interaction energy. The body of evidence on hand so far is as follows. Introduction of the cluster formation energy into the dissociative electron-transfer model has allowed a satisfactory fitting of experimental data in several cases, this finding being complemented by the observation that significant interactions are found only with radicals where strong electron-withdrawing effects are present, in line with the anticipated reinforcement of the charge/dipole attraction between the ion and the radical. The experimental examples are mostly concerned with electrochemical reactions, but one homogeneous electron-transfer example also exists.<sup>13d</sup> The reality of these interactions has been more recently confirmed through their variation with the solvent.<sup>13b</sup> It was indeed found that their magnitude decreases as the stabilization of the free ion by the solvent increases. Although the number of convergent clues is definitely growing, it is still useful to find further confirmations and particularly to examine one aspect that has not been investigated so far, namely how the interaction varies when the leaving ion changes, the radical being kept the same.

- (8) (a) Neta, P.; Behar, D. *J. Am. Chem. Soc.* **1980**, *102*, 4798. (b) Behar, D.; Neta, P. *J. Phys. Chem.* **1981**, *85*, 690. (c) Behar, D.; Neta, P. *J. Am. Chem. Soc.* **1981**, *103*, 103. (d) Behar, D.; Neta, P. *J. Am. Chem. Soc.* **1981**, *103*, 2280. (e) Bays, J. P.; Blumer, S. T.; Baral-Tosh, S.; Behar, D.; Neta, P. *J. Am. Chem. Soc.* **1983**, *105*, 320. (f) Norris, R. K.; Barker, S. D.; Neta, P. *J. Am. Chem. Soc.* **1984**, *106*, 3140. (g) Meot-Ner, M.; Neta, P.; Norris, R. K.; Wilson, K. *J. Phys. Chem.* **1986**, *90*, 168.
- (9) (a) Saeva, F. D. *Top. Curr. Chem.* **1990**, *156*, 61. (b) Saeva, F. D. Intramolecular Photochemical Electron Transfer (PET) – Induced Bond Cleavage Reactions in some Sulfonium Salts Derivatives. In *Advances in Electron-Transfer Chemistry*; Mariano, P. S., Ed.; JAI Press: New York, 1994; Vol. 4, pp 1–25. (c) Gaillard, E. R.; Whitten, D. G. *Acc. Chem. Res.* **1996**, *29*, 292.
- (10) (a) Arnold, B. R.; Scaiano, J. C.; McGimpsey, W. G. *J. Am. Chem. Soc.* **1992**, *114*, 9978. (b) Chen, L.; Farahat, M. S.; Gaillard, E. R.; Gan, H.; Farid, S.; Whitten, D. G. *J. Am. Chem. Soc.* **1995**, *117*, 6398. (c) Chen, L.; Farahat, M. S.; Gaillard, E. R.; Farid, S.; Whitten, D. G. *J. Photochem. Photobiol., A: Chem.* **1996**, *95*, 21. (d) Wang, X.; Saeva, F. D.; Kampmeier, J. A. *J. Am. Chem. Soc.* **1999**, *121*, 4364. (e) Robert, M.; Savéant, J.-M. *J. Am. Chem. Soc.* **2000**, *122*, 514. (f) Costentin, C.; Robert, M.; Savéant, J.-M. *J. Phys. Chem. A* **2000**, *104*, 7492. (g) Pause, L.; Robert, M.; Savéant, J.-M. *ChemPhysChem* **2000**, *1*, 199.
- (11) (a) Benassi, R.; Bernardi, F.; Bottoni, A.; Robb, M. A.; Taddei, F. *Chem. Phys. Lett.* **1989**, *161*, 79. (b) Bertran, J.; Gallardo, I.; Moreno, M.; Savéant, J.-M. *J. Am. Chem. Soc.* **1992**, *114*, 9576. (c) Tada, T.; Yoshimura, R. *J. Am. Chem. Soc.* **1992**, *114*, 1593.
- (12) (a) Chen, E. C. M.; Albyn, K.; Dussack, L.; Wentworth, W. E. *J. Phys. Chem.* **1989**, *93*, 6827. (b) Symons, M. C. R. *Pure Appl. Chem.* **1981**, *53*, 223. (c) Symons, M. C. R. *Acta Chem. Scand.* **1997**, *51*, 123.
- (13) (a) Pause, L.; Robert, M.; Savéant, J.-M. *J. Am. Chem. Soc.* **2000**, *122*, 9829. (b) Pause, L.; Robert, M.; Savéant, J.-M. *J. Am. Chem. Soc.* **2001**, *123*, 4886. (c) Costentin, C.; Hapiot, P.; Médebielle, M.; Savéant, J.-M. *J. Am. Chem. Soc.* **2000**, *122*, 5623. (d) Costentin, C.; Robert, M.; Savéant, J.-M., unpublished results. (e) Cardinale, A.; Gennaro, A.; Isse, A. A.; Maran, F. in *New Directions in Organic Electrochemistry*; Fry, A. J., Matsumura, A., Eds.; The Electrochemical Society, Inc.: New Jersey, 2000; Vol. 200–15, pp 136–140.

- (14) (a) Savéant, J.-M. *J. Am. Chem. Soc.* **1987**, *109*, 6788. (b) Savéant, J.-M. *J. Am. Chem. Soc.* **1992**, *114*, 10595. (c) Savéant, J.-M. *J. Phys. Chem.* **1994**, *98*, 3716. (d) Andrieux, C. P.; Savéant, J.-M.; Tardy, C. *J. Am. Chem. Soc.* **1998**, *120*, 4167.

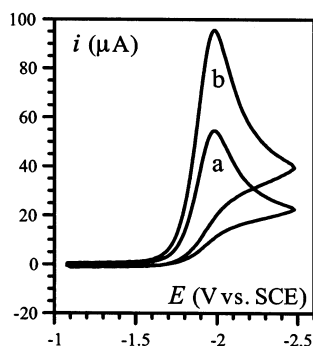


**Figure 2.** Cyclic voltammetry of 2 mM ClCH<sub>2</sub>CN in DMF + 0.1 M (*n*-C<sub>4</sub>H<sub>9</sub>)<sub>4</sub>NClO<sub>4</sub> at a glassy carbon electrode at 25 °C in the absence (a) and presence (b) of an equimolecular amount of CH<sub>3</sub>CO<sub>2</sub>H. Scan rate: 0.2 V/s.

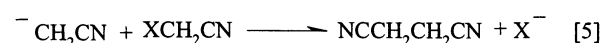
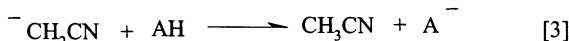
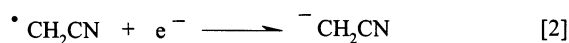
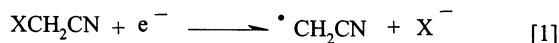
The electrochemical reduction of haloacetonitriles (chloro-, bromo-, iodo-) in a polar solvent such as DMF offers an excellent opportunity to investigate this aspect of the problem. The presence of the cyano group makes the cyanomethyl radical a good candidate for measurable interactions, allowing us to test the expectation that their magnitude should decrease when passing from Cl to Br and I. Another source of interest of this family of molecules is that, because they are small, they offer a good opportunity for detailed quantum chemical calculations that may help the understanding of their dissociative electron-transfer reactivity.

We will first ascertain, determining the reaction products and investigating the electron stoichiometry, the conditions under which the electrochemical reduction in DMF is under the kinetic control of the one-electron dissociative transfer we want to explore. A systematic investigation of the cyclic voltammetry responses as a function of the scan rate is then carried out, and the results are processed by means of the convolution technique so as to extract from the experimental data the variation of the potential-dependent rate constant over maximized ranges of driving force. The applicability of the “sticky” dissociative electron-transfer model will then be tested, and the interaction energies will be derived. The variation of their magnitude with the nature of the leaving group will then be discussed on qualitative intuitive grounds helped by some quantum chemical calculations.

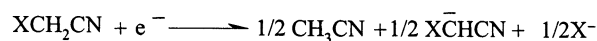
## Results

All three haloacetonitriles, XCH<sub>2</sub>CN, exhibit a single broad irreversible cyclic voltammetric peak. An example is given in Figure 2. The location of the peak strongly depends on the nature of the halide. The peak potentials (*E<sub>p</sub>*) measured, for example, at a scan rate (*ν*) of 0.2 V s<sup>-1</sup> are -2.0, -1.58, and -1.24 V versus SCE for X = Cl, Br, and I, respectively. *E<sub>p</sub>* varies linearly with the logarithm of *ν*, and the average slope, ∂*E<sub>p</sub>*/∂ log *ν*, is around 90 mV (temperature: 25 °C), while the peak width is on the order of 150 mV. These observations clearly indicate that the reaction is under the kinetic control of a slow electron-transfer step rather than of a follow-up cleavage reaction.<sup>15</sup> The radical •CH<sub>2</sub>CN obtained after the transfer of one electron and the concomitant or successive cleavage of the C–X bond (step 1 in Scheme 2) is, as many radicals formed upon reductive cleavage,<sup>15c</sup> much easier to reduce than the starting molecule.<sup>16</sup> We thus expect that the radical is immediately reduced to the acetonitrile carbanion (step 2).

**Scheme 2.** Reduction of Haloacetonitriles: Electron-Transfer Steps and Accompanying Reactions



### Electron stoichiometry resulting from the interference of father-son reactions



This is converted into acetonitrile by the strongest acid present (step 3). The haloacetonitriles may serve themselves as acids thanks to the electron-withdrawing action of the cyano group. This is what may happen (step 4) when no external acid is added to the solution. Haloacetonitriles may also serve as an electrophile in a substitution reaction where the nucleophile is the acetonitrile carbanion (step 5). The interference of the “father-son” reactions 4 and/or 5 leads to an overall one-electron-per-molecule stoichiometry, although two electrons have been exchanged.<sup>17</sup> That such reactions are indeed occurring in the present case is attested by the effect of addition of an acid such as phenol or acetic acid, which leads to a doubling of the peak height as exemplified in Figure 2 with the reduction of the chloro derivative. These results are confirmed by preparative-scale electrolysis. Controlled potential electrolyses of 45 mM solutions of XCH<sub>2</sub>CN carried out at the reduction potential of each halide consumed 1.1–1.2 e/molecule of XCH<sub>2</sub>CN, yielding CH<sub>3</sub>CN (~45%) as the main reduction product. Only trace amounts of succinonitrile were detected in these experiments. When the electrolyses were repeated in the presence of CH<sub>3</sub>CO<sub>2</sub>H, the yield of CH<sub>3</sub>CN increased to >90% with an electron consumption close to 2e/molecule of haloacetonitrile.

All further cyclic voltammetric experiments were performed in the presence of CH<sub>3</sub>CO<sub>2</sub>H. The kinetics of the electron-transfer reaction was derived from the cyclic voltammetric

- (15) (a) If the follow-up reaction is the sole rate-determining step, ∂*E<sub>p</sub>*/∂ log *ν* is much smaller and equal to 29.6 mV, and the peak width is 47.8 mV.<sup>15b,c</sup> When the first electron transfer and the follow-up reaction jointly control the kinetics, ∂*E<sub>p</sub>*/∂ log *ν* varies between 29.6 and 59.2 mV according to the respective degree of control by each step, while the peak width varies between 47.8 and 95.6 mV.<sup>15b,c</sup> (b) Nadjio, L.; Savéant, J.-M. *J. Electroanal. Chem.* **1973**, *48*, 113. (c) Andrieux, C. P.; Savéant, J.-M. *Electrochemical Reactions. In Investigations of Rates and Mechanisms of Reactions*; Bernasconi, C. F., Ed.; Wiley and Sons: New York, 1986; Vol. VI/4E, Part 2, pp 305–390.
- (16) (a) The reduction potential of •CH<sub>2</sub>CN has been estimated to be -0.86 V versus SCE in DMF,<sup>16b</sup> that is, much more positive than the reduction potentials of all three haloacetonitriles. (b) Isse, A. A.; Gennaro, A., in preparation.
- (17) (a) The interference of “father-son” reactions, particularly “self-protonation” reactions, in electrochemical mechanisms is a well-documented phenomenon.<sup>17b–e</sup> (b) Amatore, C.; Capobianco, G.; Farnia, G.; Sandonà, G.; Savéant, J.-M.; Severin, M. G.; Vianello, E. *J. Am. Chem. Soc.* **1985**, *107*, 1815. (c) Isse, A. A.; Abdurahman, A. M.; Vianello, E. *J. Chem. Soc., Perkin Trans. 2* **1996**, 597. (d) Isse, A. A.; Abdurahman, A. M.; Vianello, E. *J. Electroanal. Chem.* **1997**, *431*, 249. (e) Maran, F.; Roffia, S.; Severin, M. G.; Vianello, E. *Electrochim. Acta* **1990**, *35*, 81.



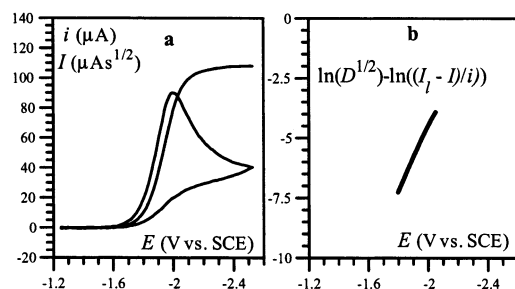


**Figure 3.** Cyclic voltammetry of 2 mM ClCH<sub>2</sub>CN in DMF + 0.1 M (*n*-C<sub>4</sub>H<sub>9</sub>)<sub>4</sub>NClO<sub>4</sub> at a glassy carbon electrode at 25 °C in the presence of an equimolecular amount of CH<sub>3</sub>CO<sub>2</sub>H at a scan rate of 0.2 V/s. (a) Construction of the convoluted current according to eq 3. (b) Logarithmic analysis according to eq 4.

curves recorded between 0.1 and 50 V/s. These were transformed by convolution of the current with the time-function  $1/\sqrt{\pi t}$ , which characterizes linear diffusion:

$$I = \frac{1}{\sqrt{\pi}} \int_0^t \frac{i(\eta)}{\sqrt{t-\eta}} d\eta \quad (3)$$

As pictured in Figure 3, the original peak-shaped curve is thus transformed into an S-shaped curve plateauing off at a value noted  $I_1$  (Figure 3). One of the most distinct advantages of the convolution method over the classical treatment of cyclic voltammograms is that the potential-dependent rate constant of electron transfer,  $k(E)$ , may be derived from the experimental data without a priori knowing the rate law of electron transfer:

$$\ln[k(E)] = \ln(\sqrt{D}) - \ln\left[\frac{I_1 - I}{i}\right] \quad (4)$$

with

$$I_1 = FSC^0\sqrt{D} \quad (5)$$

where  $S$  is the electrode surface area,  $C^0$  is the bulk concentration, and  $D$  is the diffusion coefficient.

This valuable feature of the convolution method has been the main incentive for its introduction<sup>18a,b</sup> and its application, first to outersphere electron transfers<sup>18c</sup> and, afterward, to dissociative electron transfers.<sup>4d-f,18d-g</sup> An example of the application of eq 4 is shown in Figure 3b. The same operation is repeated at each scan rate leading to overlapping  $\ln[k(E)]$  curves. The complete curves extending over the whole available potential range are shown in Figure 4 for all three derivatives. The values of the diffusion coefficient used in this treatment (Table 1) were obtained by application of eq 5.

In fact, rather than  $\ln[k(E)]$ , Figure 4 displays the variations of the corresponding activation free energy with the standard free energy of reaction after application of eq 6

$$\Delta G^\ddagger = \frac{RT}{F} \ln\left(\frac{Z}{k(E)}\right) \quad (6)$$

- (18) (a) Andrieux, C. P.; Savéant, J.-M. *J. Electroanal. Chem.* **1970**, *26*, 147. (b) Imbeaux, J. C.; Savéant, J.-M. *J. Electroanal. Chem.* **1973**, *44*, 169. (c) Savéant, J.-M.; Tessier, D. *J. Electroanal. Chem.* **1975**, *65*, 57. (d) Donkers, R. L.; Maran, F.; Wayner, D. D. M.; Workentin, M. S. *J. Am. Chem. Soc.* **1999**, *121*, 7239. (e) Severin, M. G.; Farnia, G.; Vianello, E.; Arévalo, M. C. *J. Electroanal. Chem.* **1988**, *251*, 369. (f) Isse, A. A.; Gennaro, A.; Maran, F. *Acta Chem. Scand.* **1999**, *53*, 1013. (g) Donkers, R. L.; Workentin, M. S. *J. Phys. Chem. B* **1998**, *102*, 4061.

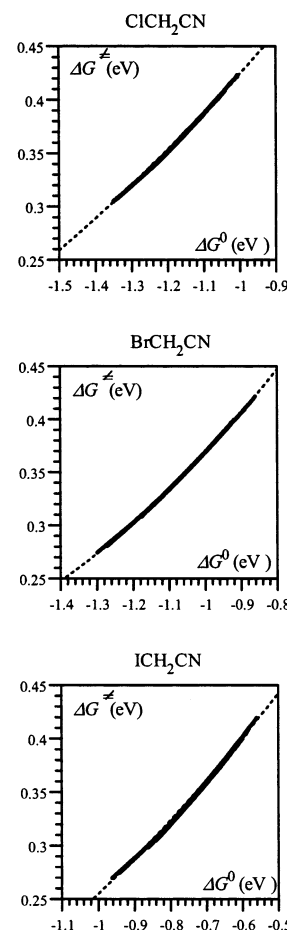


**Figure 4.** Variation of the activation free energy with the standard free energy of the reaction for the reduction of the three haloacetonitriles in DMF. Dotted line: prediction of the “sticky” dissociative electron-transfer model (see text).

**Table 1.** Diffusion Coefficients and Preexponential Factors

compound	ClCH <sub>2</sub> CN	BrCH <sub>2</sub> CN	ICH <sub>2</sub> CN
$D$ (cm <sup>2</sup> /s)	$1.36 \times 10^{-5}$	$1.29 \times 10^{-5}$	$1.19 \times 10^{-5}$
$Z$ (cm/s) <sup>a</sup>	7230	5735	4860

<sup>a</sup> Collision frequency:  $Z = \sqrt{RT/2\pi M}$  ( $M$ : molar mass).

where the preexponential factor is taken as the collision frequency on a plane,  $Z$ .<sup>14,19</sup> In the above relationship and throughout the paper, energies are in electronvolts, and potentials are in volts.

## Discussion

The smallness of the transfer coefficient ( $\alpha$  is around 0.3) not only indicates that the reaction is controlled by a slow electron-transfer step, but that this is most likely a dissociative electron-transfer process. However, application of the classical model, using eq 1, does not lead to a satisfactory fitting of the experimental data in Figure 4, the predicted activation energies being larger than the experimental ones. This discrepancy between theory and experiment increases from I to Br and to Cl. As discussed earlier, the effect of fragment clustering is to decrease the predicted activation energies. We thus now test the applicability of the “sticky” dissociative electron-transfer model, using eq 2. In fact, we used a slightly more sophisticated

- (19) Marcus, R. A. *J. Chem. Phys.* **1965**, *43*, 679.

**Table 2.** Parameters Required for Applying the Model<sup>a</sup>

X	$D_R$	$T\Delta S^\circ$	$E_{X^\cdot/X^-}^0$	$E_{RX/R^\cdot+X^-}^0$	$a_R$	$a_P$	$\lambda_0^R$	$\lambda_0^P$	$D_P$
Cl	2.88	0.3	1.81	-0.77	2.93	1.81	1.02	1.66	<b>39</b>
Br	2.26	0.3	1.48	-0.48	3.02	1.96	0.99	1.53	<b>7</b>
I	1.67	0.3	0.99	-0.38	3.06	2.20	0.98	1.36	<b>2.5</b>

<sup>a</sup> Energies in electronvolts (except  $D_P$ , in millielectronvolts), potentials in volts versus SCE, radii in angstroms.

version of the model in which provision is made for a variation of the solvent reorganization factor as the reaction proceeds. In the simpler version, the solvent reorganization energy,  $\lambda_0$ , is considered as a constant in eqs 7 and 8 defining the free energy profiles,  $G_R$  and  $G_P$ , of the reactant and product systems, respectively.

$$G_R = D_R Y^2 + \lambda_0(Y) X^2 \quad (7)$$

$$G_P = \Delta G^0 - D_P + D_R \left( 1 - \sqrt{\frac{D_P}{D_R}} - Y \right)^2 + \lambda_0(Y)(1 - X)^2 \quad (8)$$

$X$  is a nominal charge borne by the molecule, varying from 0 to 1, serving as the index for solvent reorganization.

$$Y = 1 - \exp[-\beta(y - y_{RX})]$$

with  $\beta = \nu(2\pi^2\mu/D_R)^{1/2}$  ( $y$ , bond length;  $y_{RX}$ , equilibrium value of  $y$  in the reactant system;  $\nu$ , frequency of the cleaving bond;  $\mu$ , reduced mass;  $D_R$ , bond dissociation energy of the starting molecule) serving as the index for bond breaking.

$\Delta G^0 = E - E_{RX/R^\cdot+X^-}^0$  is the standard free energy of the reaction ( $E$ , electrode potential;  $E_{RX/R^\cdot+X^-}^0$ , standard potential of the  $RX/R^\cdot + X^-$  couple).

$D_P$  is the interaction energy that is the object of our investigation.

In the advanced version we use here, the solvent reorganization energy is assumed to vary with the degree of bond breaking according to eq 9.

$$\lambda_0(Y) = (1 - Y)\lambda_0^R + Y\lambda_0^P = \lambda_0^R + (\lambda_0^P - \lambda_0^R)Y \quad (9)$$

where  $\lambda_0^R$  is the solvent reorganization energy that corresponds to the charge being spread over the entire molecule as in the reactant system, while  $\lambda_0^P$  corresponds to the charge being located on the leaving anion as in the product system.

It follows that the activation free energy is obtained as a function of  $\Delta G^0$  from eq 10 after extraction of  $X^\ddagger$  and  $Y^\ddagger$  from eqs 11 and 12.

$$\Delta G^\ddagger = D_R Y^{\ddagger 2} + [\lambda_0^R + (\lambda_0^P - \lambda_0^R)Y^\ddagger] X^{\ddagger 2} \quad (10)$$

$$Y^\ddagger = \left( 1 - \sqrt{\frac{D_P}{D_R}} \right) X^\ddagger - \frac{\lambda_0^P - \lambda_0^R}{2D_R} X^{\ddagger 2} (1 - X^\ddagger) \quad (11)$$

$$\Delta G^0 = D_P + D_R \left( 1 - \sqrt{\frac{D_P}{D_R}} \right) \left[ 2Y^\ddagger - \left( 1 - \sqrt{\frac{D_P}{D_R}} \right) \right] + [\lambda_0^R + (\lambda_0^P - \lambda_0^R)Y^\ddagger] (2X^\ddagger - 1) \quad (12)$$

Application of the model requires the knowledge of a series of parameters, the values of which are listed in Table 2, that were obtained as follows.

The C–Cl bond dissociation energy in  $ClCH_2CN$  is 2.88 eV.<sup>20</sup> The C–X bond dissociation energies of the bromo and iodo derivatives are not known. From the bond dissociation energies of various alkyl halides  $RX$  ( $X = Cl, Br, I$ ) reported in the literature,<sup>20</sup> it can be inferred that, although they depend on the structure of the alkyl group, for any given  $R$ , the difference between the values for C–Cl and C–Br is about constant and equal to  $0.62 \pm 0.06$  eV on average. Likewise, the difference between the values for C–Cl and C–I is about constant and equal to  $1.21 \pm 0.12$  eV on average. The values reported in Table 2 ensue.

The ingredients required to estimate the standard potential of the  $RX/R^\cdot + X^-$  couple are indicated in eq 13:

$$E_{RX/R^\cdot+X^-}^0 = -D_R + T\Delta S^\circ + E_{X^\cdot/X^-}^0 \quad (13)$$

where  $\Delta S^\circ$  is the bond dissociation entropy. Concerning this factor, it is important to note that the standard values calculated in the gas phase have to be corrected for the change in the standard state when passing from the gas to the liquid phase (1 atm and 1 mol/L, respectively), which amounts to decreasing each of the values obtained by  $R/F \ln(22.4)$ , that is, 0.268 meV/(mol K). This leads to an entropic contribution,  $T\Delta S^\circ$ , of about 0.3 eV (based on quantum chemical calculations). The standard potentials for oxidation of the halides were taken from the literature.<sup>13a,14c</sup> The standard potentials thus deduced from eq 13 are listed in Table 2.

The solvent reorganization energies are derived from the corresponding radii of the equivalent spheres according to  $\lambda_0$  (eV) =  $3/a$  (Å),<sup>14b,d</sup> leading to the values listed in Table 2.

All necessary parameters are now gathered for performing the resolution of eqs 10–12 for each derivative, adjusting the value of the interaction energy,  $D_P$ , so as to obtain the best fit of the experimental data. As can be seen in Figure 4, an excellent fit is achieved for the values of  $D_P$  reported in the last column of Table 2. The extreme sensitivity of  $\Delta G^\ddagger$  to changes in the  $D_P$  values allowed a quite precise determination ( $\pm 2\%$ ) of the interaction energy.

We are thus led to conclude that dissociative electron transfer to all three haloacetonitriles follows a concerted rather than stepwise mechanism leading to a cluster of weakly interacting fragments. It is remarkable that the strength of the interaction rapidly decreases from the Cl to the Br and to the I derivative. In this connection, it is interesting to note the existence of a correlation between the interaction energy and the radius of the leaving anion (Figure 5a).

This observation points to the notion that the interaction in the fragment cluster is essentially electrostatic in nature.

We have then performed a series of quantum chemical calculations (see the Methodology for the Quantum Chemical Calculations section) for confirming and illustrating these conclusions. The gas-phase energy versus C–X distance profiles are shown in Figure 6 together with the optimized geometry of the energy minimum and its main distance, charge, and spin density characteristics. A clear energy minimum is found in all cases. In all corresponding structures, the carbon–halogen distance (Figure 6) is large, much larger than that in the parent molecule. This observation confirms that the fragment cluster

(20) NIST Standard Reference Database 25. *NIST Structures and Properties Database and Estimation Program*, 1991; U.S. Department of Commerce: Gaithersburg, MD 20899, 1991.

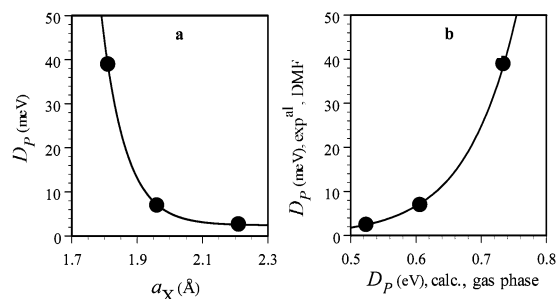


**Figure 5.** Correlation between the experimental interaction energies in the fragment clusters in DMF and the radii of the leaving halide ions (a), or the calculated interaction energies in the gas phase (see text) (b).

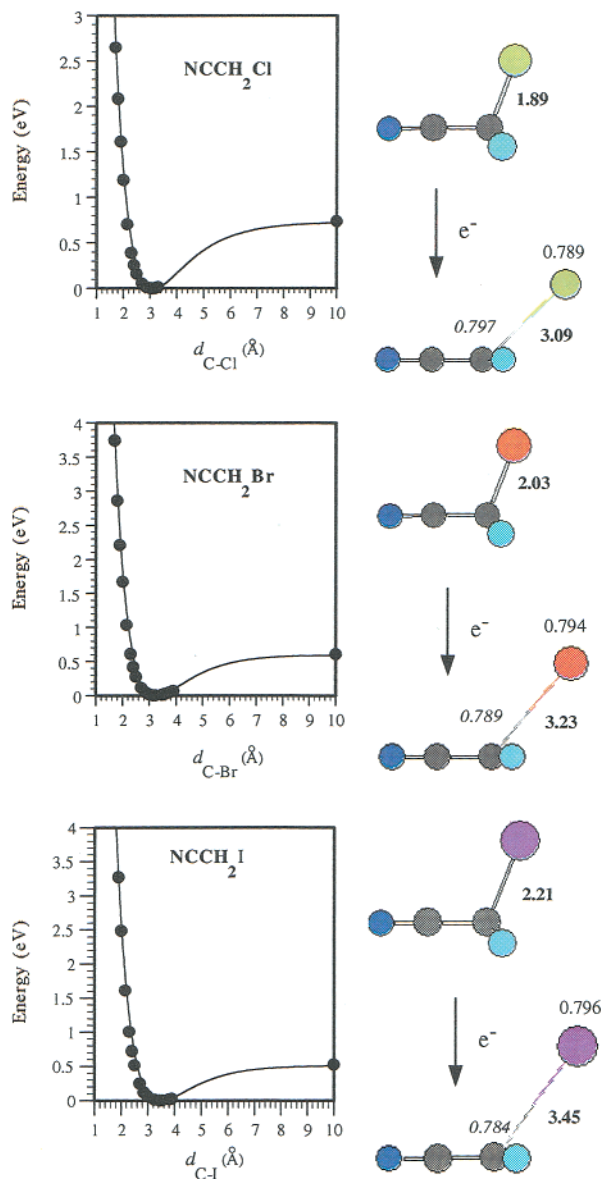


**Figure 6.** Left: calculated (B3LYP/CEP-121G) potential energy profiles for  $(-X, \cdot CH_2CN)$  in the gas phase. Right: optimized geometries (B3LYP/CEP-121G) of  $XCH_2CN$  and  $(-X, \cdot CH_2CN)$  in the gas phase. Bold numbers: C-X distance in Å. Plain numbers: fraction of the negative charge borne by the halogen atom. Italic numbers: spin density on the carbon atom of the cleaving bond.

is not a radical ion but is rather an electrostatic ion-radical pair. The fact that about 80% of the negative charge stands on the halogen atom while 80% of the spin density is located on the

facing carbon atom (Figure 6) is an additional argument in favor of this conclusion. It should be emphasized that the profiles do not show any trace of a local minimum, or inflection point, at shorter distances that could have been the sign of an unstable true radical ion.

It is also worth noting that the energy of interaction decreases from Cl to Br and to I as it does in DMF (Figure 5b). Its values are considerably smaller in the solvent than in the gas phase, and the variation is more rapid in the first case than in the second, in line with the strong solvation of the halide ions by the solvent. Attempts to mimic the effect of solvation by dielectric continuum models such as COSMO (see the Methodology for the Quantum Chemical Calculations section) were unsuccessful in the sense that a complete disappearance of the energy minima occurred in all three cases. This is actually not too surprising because dielectric continuum models are anticipated to overestimate ion solvation and because the rather tenuous interaction we are dealing with is too subtle for the present accuracy of ab initio techniques.

## Conclusions

Our main conclusions are as follows:

(i) The reductive cleavage of the three haloacetonitriles in DMF provides additional examples of the formation of a fragment cluster upon dissociative electron transfer. The fact that the interaction energies in the radical-ion pair thus formed are measurable despite the polar character of the solvent is the result of the electron-withdrawing character of the cyano group borne by the carbon atom of the breaking bond.

(ii) It was confirmed that small interaction energies result in large changes in the activation energies. This remarkable sensitivity allows, with help of the “sticky” dissociative electron-transfer model, the precise determination ( $\pm 2\%$ ) of interaction energies down to a few millielectronvolts from the cyclic voltammetry of the reductively cleaving substrate.

(iii) The interaction energy rapidly decreases from Cl to Br and to I and shows a decreasing correlation with the halide radius. This observation adds to the previously gathered evidence (favoring influence on the kinetics of dissociative electron transfer, assisting role of electron-withdrawing groups on the radical, effect of changing the solvent) to confirm the existence of such interactions and to highlight their electrostatic character.

(iv) The formation of an electrostatic, endothermically cleaving radical-ion pair rather than of an exothermically cleaving true anion radical is further confirmed by the quantum chemical computation of the potential energy profiles, which exhibit a long-distance energy minimum. Not only is the carbon-halogen distance far too large for a true anion radical, but its radical-ion pair character is confirmed by the fact that the halogen bears 80% of the negative charge and that 80% of the spin is located on the carbon atom of the breaking bond. Although the experimental interaction energies are much smaller than their computed gas-phase counterparts, they both decrease in a correlated manner from Cl to Br and I. As expected, the carbon-halogen distance increases correlatively.

(v) The present work and the preceding studies of the in-cage interactions between radicals and ion may be regarded as a revisiting of the notion of  $\sigma$ -ion radicals and of their status in a polar medium. They thus appear as an electrostatic radical-ion pair rather than covalently bound molecules. Their stability

is a function of the Lewis acid–base properties of both the radical and the leaving ion and is strongly influenced by the nature of the solvent.

## Experimental Section

**Chemicals.** DMF (Janssen, 99%) was kept over anhydrous  $\text{Na}_2\text{CO}_3$  for several days and stirred from time to time. It was then fractionally distilled under reduced pressure under  $\text{N}_2$  twice and stored in a dark bottle under  $\text{N}_2$ . Tetra-*n*-butylammonium perchlorate (Fluka 98%) was recrystallized twice from a 2:1 water–ethanol mixture and dried at 60 °C under vacuum. The haloacetonitriles were all commercially available and were used as received.

**Instrumentation.** The electrochemical measurements were made with a PAR Model 173 potentiostat, a PAR 175 universal programmer, a Nicolet 3091 12-bit resolution digital oscilloscope, and an Amel 863 X/Y pen recorder. In most of the experiments, the cyclic voltammograms were recorded for scan rates ranging from 0.1 to 50  $\text{V s}^{-1}$  (first in the absence and then in the presence of the haloacetonitrile) by the digital oscilloscope (digitalized 1 point/mV) and then transferred to a PC. The background-subtracted curves were then transformed by convolution with the function  $1/(\pi t)^{1/2}$ . All experiments were conducted in a three-electrode all-glass cell, thermostated at 25 °C. A glassy carbon (Tokai GC-20) electrode, prepared and activated before each measurement as previously described,<sup>18f</sup> was used as the working electrode, and a platinum wire was used as the counter electrode. The reference electrode was  $\text{Ag}/\text{AgI}/\text{Bu}_4\text{NI}$  0.1 M DMF, calibrated after each experiment against the ferrocene/ferricinium couple. The standard

potential for ferrocene oxidation in DMF + 0.1 TBAP is 0.475 V against the KCl saturated calomel electrode (SCE). Throughout the paper, all of the potential values will be reported against SCE. Controlled potential electrolyses were carried out in a divided cell by using a carbon rod electrode. Gas chromatographic analysis of the electrolysis products was performed with a Varian 3700 chromatograph equipped with a 10% Carbowax 20M on Supelcoport (80–100 mesh) column.

**Methodology for the Quantum Chemical Calculations.** All of the calculations were performed with the Gaussian 98 series of programs.<sup>21</sup> Different methods were used for the chloro derivative: DFT (B3LYP) and Hartree–Fock with Möller–Plesset perturbation (MP2). The 6-31G\* basis set was used as well as CEP-121G (at the B3LYP level of calculation). Minimum energy structures were fully optimized, and frequency calculations were made to verify that the structures were minima (no imaginary frequencies) on the potential energy surface. DFT and MP2 calculations give similar results in terms of C–Cl distance and charge repartition; DFT calculations were preferred because of some spin contamination at the MP2 level. The basis set used has almost no effect on the DFT results.

Calculations on the two other bromo and iodo derivatives were then performed at the B3LYP/CEP-121G level. Energy profiles were obtained at various lengths of the C–X bonds for the three parent molecules plus one electron. The energy of the separated fragments was obtained by adding the energies of the leaving anion  $\text{X}^-$  and radical  $\text{NCCH}_2^\cdot$ . Partial negative charge on the halogen atom was obtained by a Mulliken population analysis. All along the gas-phase profile, free energies of solvation were also evaluated using the COSMO procedure (conductor-like screening model), which is a continuum approach generating a polygonal surface around the system at the van der Waals distance. The energy at the infinite separation of the two fragments was obtained by adding the solvation free energies of  $\text{X}^-$  and  $\text{NCCH}_2^\cdot$ .

**Acknowledgment.** This work was financially supported in part by the Consiglio Nazionale delle Ricerche (CNR) and the Ministero dell'Istruzione, dell'Università e della Ricerca (MIUR), Italy.

JA0275212

- (21) Frisch, M. J.; Trucks, G. W.; Schlegel, H. B.; Scuseria, G. E.; Robb, M. A.; Cheeseman, J. R.; Zakrzewski, V. G.; Montgomery, J. A., Jr.; Stratmann, R. E.; Burant, J. C.; Dapprich, S.; Millam, J. M.; Daniels, A. D.; Kudin, K. N.; Strain, M. C.; Farkas, O.; Tomasi, J.; Barone, V.; Cossi, M.; Cammi, R.; Mennucci, B.; Pomelli, C.; Adamo, C.; Clifford, S.; Ochterski, J.; Petersson, G. A.; Ayala, P. Y.; Cui, Q.; Morokuma, K.; Malick, D. K.; Rabuck, A. D.; Raghavachari, K.; Foresman, J. B.; Cioslowski, J.; Ortiz, J. V.; Stefanov, B. B.; Liu, G.; Liashenko, A.; Piskorz, P.; Komaromi, I.; Gomperts, R.; Martin, R. L.; Fox, D. J.; Keith, T.; Al-Laham, M. A.; Peng, C. Y.; Nanayakkara, A.; Gonzalez, C.; Challacombe, M.; Gill, P. M. W.; Johnson, B. G.; Chen, W.; Wong, M. W.; Andres, J. L.; Head-Gordon, M.; Replogle, E. S.; Pople, J. A. *Gaussian 98*, revision A.1; Gaussian, Inc.: Pittsburgh, PA, 1998.